PERFORMANCE OPTIMIZATION OF LARGE STROKE FLEXURE HINGES FOR HIGH STIFFNESS AND EIGENFREQUENCY

K. Gunnink, R.G.K.M Aarts, and D.M. Brouwer
Mechanical Automation and Mechatronics
University of Twente, Enschede, The Netherlands

ABSTRACT

Two flexure hinge types are optimized for high support stiffness and high first unwanted eigenfrequency for two different working ranges, ±5.7° and ±20°. We show how multiple performance specifications lead to different designs with different performance. The optimization uses efficient parameterized non-linear beam-based models. The constraints and load case are taken from an electron microscopy use case.

Optimization results show that the Three Flexure Cross Hinge has the highest first unwanted eigenfrequencies, while the new Infinity Flexure Hinge shows highest support stiffnesses. The design of the optimal geometry is detailed such that a prototype mechanism is manufactured and tested. Experiments show that the first unwanted eigenfrequency is 35 times higher than the first eigenfrequency throughout the working range.

INTRODUCTION

Precision mechanisms often use flexure based hinges for their deterministic behavior and the absence of friction, stiction and backlash. Motion in vacuum is easily enabled without contamination by particles. However, the initially high support stiffness decreases rapidly with deflection. Therefore, sound conceptual designs need to be optimized for stiffness and eigenfrequency over the range of motion with limited stress, actuation stiffness and in a confined volume. The dimensions of the flexures will strongly affect the occurring stresses and performance, making it complex and time-consuming to find the optimal parameters. Chen and Howell [1] proposed a thickness-to-width ratio independent analytical method, but this method is only applied to notch hinges. With more complex shapes, such as the Cross-spring Pivot [2], here called Three Flexure Cross Hinge (TFCH), a numerical method based on a parametric model is preferred to find the optimal design. Boer et al. [3] use a multibody modeling approach, applied to the Curved Hinge Flexure, with which accurate results are obtained for the stiffness characteristics and maximum occurring stresses. Wiersma et al. [4] proposed a method to investigate the performance of several flexure hinge types for large deflection. The new Infinity Flexure (∞-FH, shown in Figure 1) appeared to have the highest first unwanted eigenfrequency over a ±20° range of motion. The compliant actuation direction causes the lowest eigenfrequency. Therefore, the first unwanted eigenfrequency is the second; f_2. However, only one load case with a large moment of inertia and a single optimization criterion, the first unwanted eigenfrequency, were used.

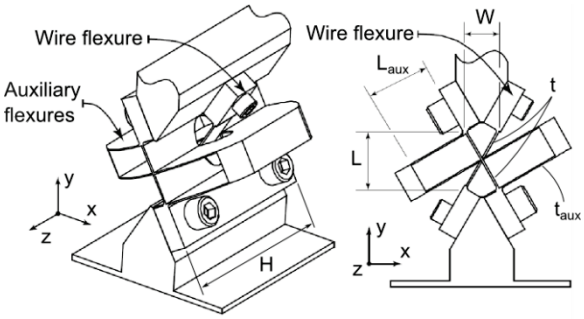

Figure 1. Parameterization of the ∞-FH [4].

This paper extends the method by researching the influence of a different load case, two optimization criterions and the influence of optimizing for different ranges of motion. The TFCH and the ∞-FH, the flexures that showed the best performance [4], are compared.

OPTIMIZATION METHOD

The optimization method starts by defining optimization criteria. Secondly an optimization routine with cost function and constraints should be set-up. Next a sufficiently accurate and fast flexure model is required. The initial geometry is based on sound designs in this case originating from Wiersma [4].

OPTIMIZATION CRITERIA

The optimization criteria are based on an electron microscopy device case. The stiffness at point *T*, Figure 2, and the first unwanted eigenfrequency are of importance. Figure 2

shows a schematic overview of the hinge and load case in undeflected position. The hinge rotates about the origin and is on one side fixed, while on the other side a body is attached. This body is assumed to be rigid and has its center of mass at point *C*. In this point, the mass of the rigid body *m* and inertia, detailed in Table 1, are attached. In point *T*, at a distance *R* = 50 from the origin, a tool can be attached, such that the support stiffness at this location is important. Point *C* is fixed with respect to *T*. The dimensions of the hinge and rigid connection to point *C* can be varied in the optimization. The hinge has Inconel 718 flexures with a Young's modulus of 210 GPa. The hinge orientation line is used to orient the hinge with respect to the load in point *T*, as parameterized by the angle ϕ. Finally, θ is the deflection angle of the hinge.

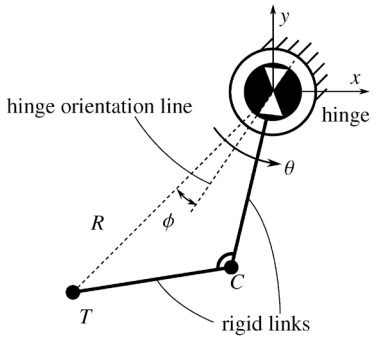

Figure 2. Schematic overview of the mechanism and load case.

Table 1. Loadcase parameters.

Parameter	Value	Unit
m	0.100	kg
J_{xx}	$21.8 \cdot 10^{-6}$	$kg \cdot m^2$
J_{xy}	$-4.88 \cdot 10^{-6}$	$kg \cdot m^2$
J_{xz}	$-3.48 \cdot 10^{-6}$	$kg \cdot m^2$
J_{yy}	$18.0 \cdot 10^{-6}$	$kg \cdot m^2$
J_{yz}	$-3.22 \cdot 10^{-6}$	$kg \cdot m^2$
J_{zz}	$19.8 \cdot 10^{-6}$	$kg \cdot m^2$

OPTIMIZATION ROUTINE

In order to maximize the support stiffness or first unwanted eigenfrequency, two cost functions are minimized in two separate optimization runs. Firstly, the hinges are uni-directionally optimized for stiffness in *z*-direction c_z at point *T*, for the deflection angles +5.7° and +20°. Secondly, for the first unwanted eigenfrequency the hinges are optimized for bi-directional ranges of motion of ±5.7° and ±20°. In order to obtain a manufacturable design with restricted dimensions, the non-linear constraint function includes limits on the Von Mises stress to 600 MPa and the actuation moment to 6 Nm. A lower limit is set for the first unwanted eigenfrequency f_2 > 300 Hz in the full working range. The optimization algorithm needs to deal with non-linear constraints and since the derivatives of the parameter set are unknown a derivative free algorithms is required. A suitable algorithm presented by Nelder and Mead [5] is modified such that the parameter vector is discarded if the constraint function is violated.

FLEXURE MODEL

The optimization requires a parameterized model. In order to keep the computation time within bounds, an efficient modeling approach is required. While Finite Element methods are accurate and widely used, models require large numbers of elements in order to handle the displacements and deformations accurately. Therefore we used models that are based on a flexible multibody approach called SPACAR with non-linear finite beam elements such that it can capture the geometric non-linear behavior with a small number of elements and relatively low computation times [6]. The flexure dimensions (short and wide) do not match well with the assumptions of Euler beam theory, so we modified the torsion stiffness of the beams to account for constrained warping [4]. We used ANSYS APDL and ANSYS Workbench to validate the results from SPACAR. For an experimental validation, a prototype is built. It includes actuators and sensors and has to be vacuum compatible. Measurement data and simulation results are compared in order to verify the optimization and performance of the hinges.

DESIGN 1: THREE-FLEXURE CROSS HINGE

For both hinge types, a suitable parameter vector is presented and parameter bounds are provided, such that the optimal geometry is manufacturable and its volume confined. The parameterized geometry of the TFCH is shown in Figure 3. The parameter vector to optimize is given by {*L w t* h_0 ϕ}, where *L* and *w* are the length and width of the hinge and *t* the thickness of the three flexures. The hinge height *H* is fixed to 54 mm, such that using the outer flexure height h_0 as parameter is sufficient to describe the height of all three flexures. The hinge orientation angle ϕ is the angle between the direction of the outer flexures and point *T*, see Figure 2. The lower and upper parameter bounds, summarized in Table 2, are required in order to obtain a feasible solution.

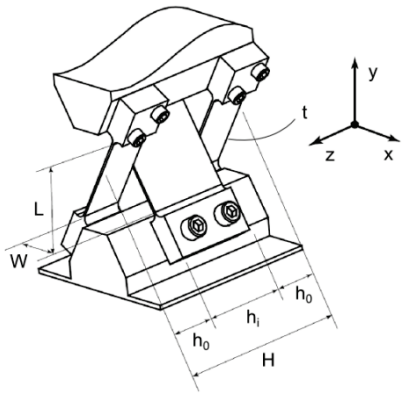

Figure 3. Parameterization of the TFCH [4].

Table 2. Parameter bounds for the TFCH.

Parameter	L	w	t	h_0	ϕ
	mm	*mm*	*mm*	*mm*	°
Lower bound	10	6	0.2	8	-30
Upper bound	40	15	0.7	15	30

The optimal geometries for the TFCH are determined for highest support stiffness and highest first unwanted eigenfrequency. These geometries are shown in Figure 9. The varying results over the range of motion are shown in Figure 4 and Figure 5. Table 3 summarizes the performance of the optimal hinges. The maximum Von Mises stress showed to be the critical constraint in all cases and is therefore not mentioned. The required actuation moment M is significantly lower for the eigenfrequency optimization at θ_{opt}= 5.7°.This is a result of the shorter and thinner flexures, see Figure 9(b).

Table 3. Performance of the optimal TFCH geometries. M is the actuation moment required for the full stroke θ_{max}, while c_z and f_2 values are measured at θ_{opt}.

Criterion	θ_{opt}	M	c_z	f_2
	°	Nm	N/m	Hz
c_z	5.7	1.42	$8.50 \cdot 10^6$	507
f_2	5.7	0.38	$6.81 \cdot 10^6$	1619
c_z	20	1.56	$2.31 \cdot 10^6$	528
f_2	20	1.52	$1.35 \cdot 10^6$	836

DESIGN 2: INFINITY-FLEXURE HINGE

The ∞-Flexure Hinge is shown in Figure 1. The parameter vector describing this hinge is {L w t L_{aux} t_{aux} ϕ}. The hinge orientation angle ϕ is the angle direction of the main flexure and point T, see Figure 2. The parameter bounds for the ∞-FH are summarized in Table 4.

The optimal geometry for the ∞-FH is determined for highest support stiffness and highest first unwanted eigenfrequency. The results are shown in Figure 10 and summarized in Table 5. In order to reduce computation times only several parameters are included in the optimization parameter vector. The auxiliary body height converged to 42 mm. The thickness of the wire flexure t_w was approximately equal to the main flexure thickness t. The wire height h_w was set at 15 mm, which is reasonable compromise between lateral stiffness of the flexure and loss of c_z stiffness due to a hole in the main flexure. The auxiliary bodies of the hinge have a thickness of t_1, which was optimized in a second optimization.

Table 4. Parameter bounds for the ∞-FH.

Parameter	L	w	t	L_{aux}	t_{aux}	ϕ
	mm	mm	mm	mm	mm	°
Lower bound	25	10	0.4	20	0.3	-30
Upper bound	45	25	0.7	40	0.7	30

Table 5. Performance of the optimal ∞-FH geometries. M is the actuation moment required for the full stroke θ_{max}, while c_z and f_2 values are measured at θ_{opt}.

Criterion	θ_{opt}	M	c_z	f_2
	°	Nm	N/m	Hz
c_z	5.7	2.74	$11.8 \cdot 10^6$	436
f_2	5.7	1.62	$3.5 \cdot 10^6$	542
c_z	20	5.05	$5.6 \cdot 10^6$	327
f_2	20	3.37	$3.8 \cdot 10^6$	438

INFLUENCE OF OPTIMIZATION CRITERIA

Figure 4 and Figure 5 show the support stiffness and first unwanted eigenfrequency respectively, for the full stroke of ±20°. The solid lines correspond with stiffness optimizations, whereas the dashed lines correspond with eigenfrequency optimizations. The influence of the criterion is clearly visible, since the stiffness of an eigenfrequency optimization is significantly lower than for the case when this stiffness was the optimization goal. For example, the first unwanted eigenfrequency f_2 of the TFCH optimized with θ_{opt} =5.7° is about 50% higher for the f_2 optimization over almost the entire stroke.
The results of this research demonstrate clearly that the optimization criterion is of major importance for the resulting optimal geometry. Hence, it should be specified clearly in view of the design requirements.

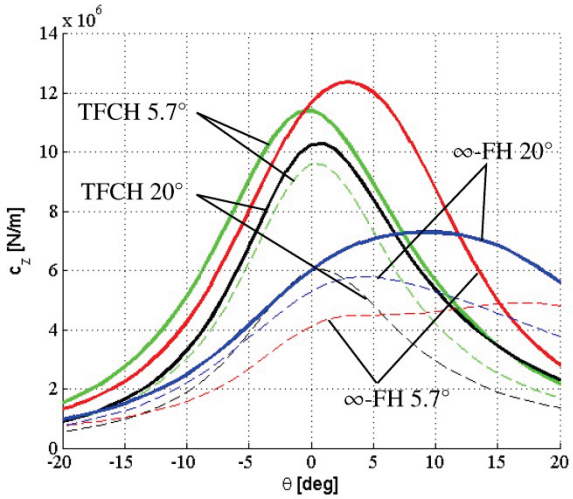

Figure 4. TFCH and ∞-FH stiffness results.

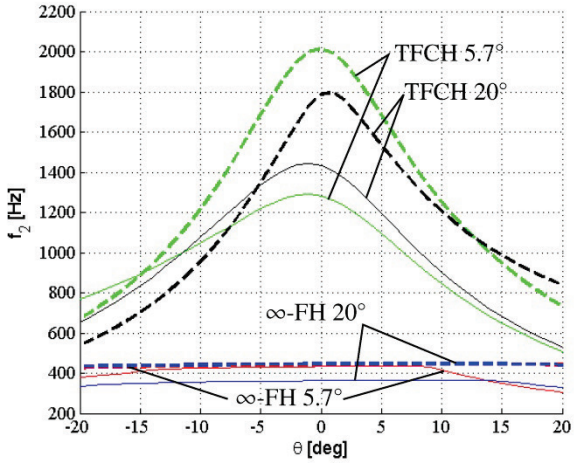

Figure 5. TFCH and ∞-FH first unwanted eigenfrequency results.

With respect to the optimal geometric designs, Figure 9 and Figure 10, we can conclude:
-The optimized geometries of the TFCH are smaller than the ∞-FH.
-The optimization of eigenfrequency leads to smaller designs than the optimization for stiffness
-The point where the stiffness is optimized is close to collinear with the main flexure of the ∞-FH and the outer flexures of the TFCH ($|\phi|<12°$).
-Due to low frequency internal modes of the auxiliary flexures the optimization for eigenfrequency of the ∞-FH leads to smaller auxiliary flexures than optimizing for stiffness. Larger auxiliary flexures allow thicker auxiliary flexures which are crucial for torsional stiffness and therefore for stiffness at $\theta = 5.7°$ or 20°.

- The asymmetric shape of the support stiffness lines of the ∞-FH shows that this flexure can be tuned to a specific load case very well. Alternatively, the TFCH design is less susceptible to optimization criteria changes than the ∞-FH.
-Optimization for stiffness or eigenfrequency leads to local compliance flexure designs as opposed to distributed compliance. This is proven by the fact that none of the optimizations was limited by the upper bound on the length parameter.
-Optimizing for $\theta = 5.7°$ leads to smaller designs than for $\theta = 20°$.

EXPERIMENTAL VALIDATION

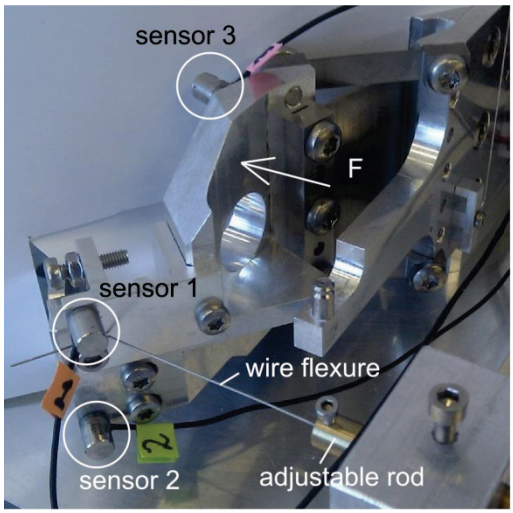

Figure 6. Measurement setup for investigation of the effects of a deflected hinge. The accelerometers are encircled and the direction of the impact force F is shown.

The eigenfrequencies of the prototype were measured in order to verify the simulation results. The prototype was placed on an isolated table and tested using three accelerometers and a small impact hammer. Figure 6 shows the locations of the three accelerometers, which measure the acceleration perpendicular to the face to which they are attached. The location and direction of the impact hammer force is shown as well. The shown wire flexure can be used to constrain the actuation direction, but is not used in this paper. Figure 7 shows the FFT-data of the measurements, from which it can be seen that the actuation frequency and both torsion modes are dominant. The large peak at 50Hz for the hammer data and the small peaks at 150 and 250Hz for the measurement of sensor 3 are artifacts of the AC power supply.

The relative amplitudes and phase data of the sensors match with the predicted eigenmodes. The measured eigenfrequencies are summarized in Table 6. The second column of shows the results from SPACAR. The third column summarizes the ANSYS APDL results based on a model using SHELL 281 elements for the flexures and MPC184 elements for the rigid bodies. The FEM analysis of the detailed design is done with ANSYS Workbench and summarized in the fourth column. The last column shows the experimental results.
The models in SPACAR and ANSYS APDL are limited to the flexure design with rigid load and base. The model in ANSYS Workbench contains the finite stiffness of the base and actuated body, where the confined available volume limits the possibilities to increase the stiffness. This gives rise to an extra mode, Figure 8. Therefore the SPACAR and ANSYS APDL results match, and the experimental results confirm the extra mode predicted by ANSYS Workbench.

Table 6. Comparison of eigenfrequency results (in Hz) at $\theta = 0$

Mode	SPACAR	ANSYS APDL	ANSYS Workbench	Exp.
1	28.0	28.2	27.6	29
2	1996	1636	1196	1040
3	2872	2910	1586	1289

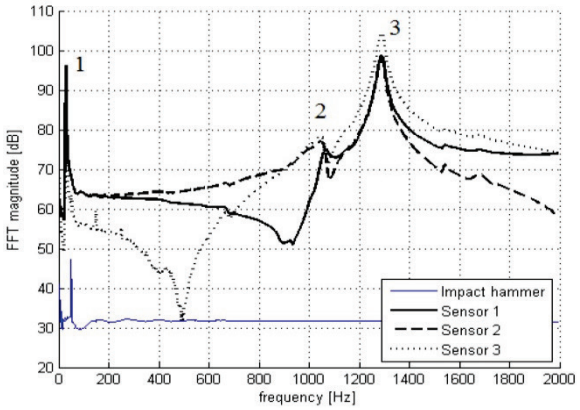

Figure 7. FFT magnitude data. The numbered peaks correspond with the frequencies in Table 6.

CONCLUSION

In this paper, a method is presented for the design and optimization of flexure hinges for large stroke use cases. The influence of the optimization criterion is significant. The trade-off between support stiffness and first unwanted eigenfrequency yields different optimal geometries.

Two hinge types, the Three Flexure Cross Hinge and Infinity Flexure have been analyzed using the presented method. The ∞-FH improves the support stiffness of the system, but a larger volume is required. Furthermore, the internal eigenfrequencies are significantly lower than for the TFCH. The optimization angle can be fine-tuned to perform optimally for specific deflection angles.
Measurements of the manufactured prototype match well with the detailed analysis performed with ANSYS Workbench. Apart from the inherent limitations the modeling and optimization proved to be very attractive for the design of the flexure hinges.

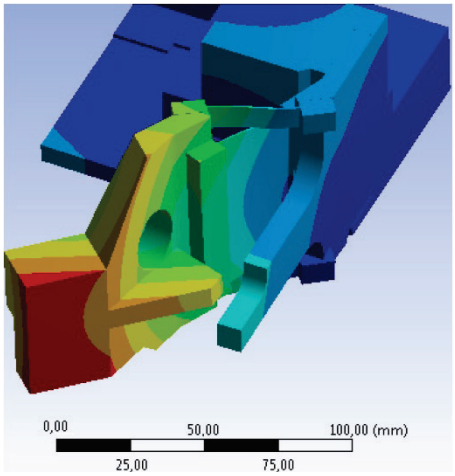

Figure 8. Total deformation plot of the second eigenmode as predicted by the Ansys Workbench analysis of the detailed model.

REFERENCES

[1] G. Chen, L. Howell. Two general solutions of torsional compliance for variable rectangular cross-section… Prec. Eng. 2009; 33: 268-274.
[2] J. Haringx. The cross-spring pivot as a constructional element. Applied Scientific Research. 1949; 1: 313-332.
[3] S. Boer et al. Multibody modelling and optimization of a curved hinge flexure. Int. conf. on multibody syst. dyn. 2010.
[4] D. Wiersma, et al. Performance optimization of large stroke spatial flexure hinges. J. Comp. Nonlin. Dyn. Submitted.
[5] J. A. Nelder, R. Mead, A simplex method for function minimization, The Computer Journal 7 (1965) 308–313.
[6] J. B. Jonker, J. P. Meijaard, Spacar - computer program for dynamic..., in: Multibody Systems Handbook, Springer-Verlag, Berlin, 1990, 1990, pp. 123–143.

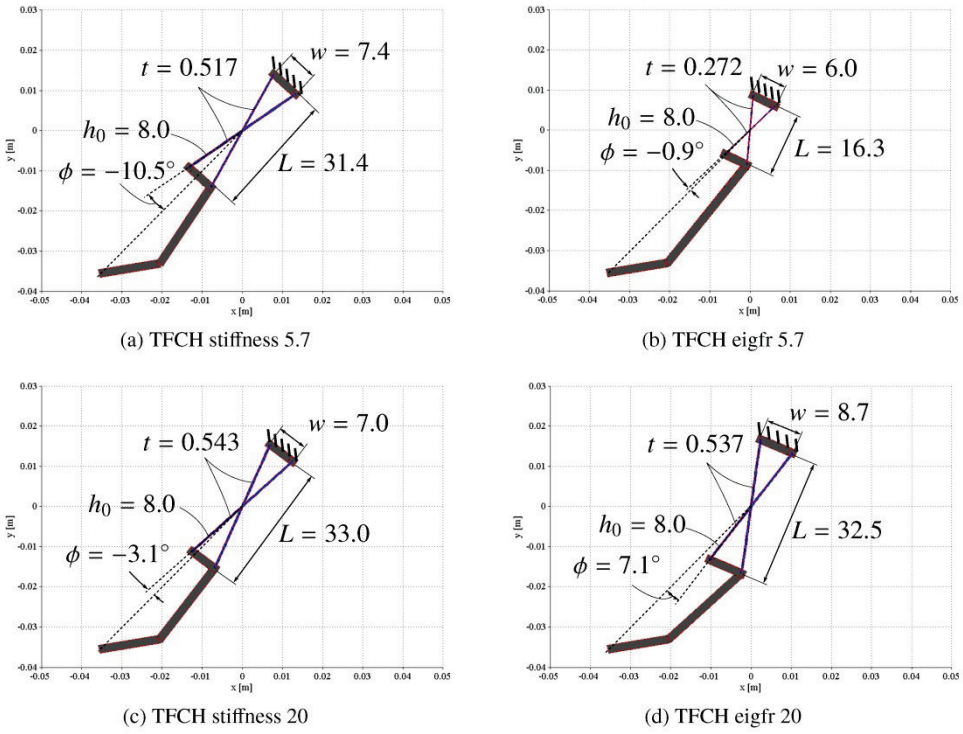

Figure 9. Optimal TFCH geometries for stiffness (left), eigenfrequency (right), 5.7° (top) and 20° (bottom) range of motion. All dimensions in mm. ϕ is the angle between the load and the outer flexures.

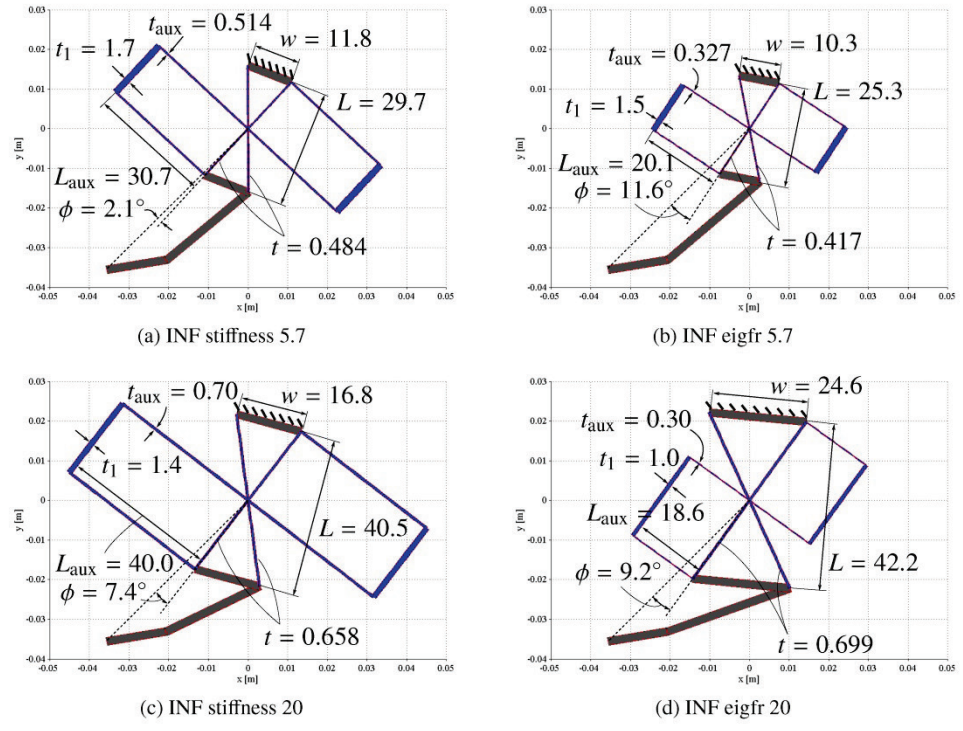

Figure 10. Optimal ∞-FH geometries for stiffness (left), eigenfrequency (right), 5.7° (top) and 20° (bottom) range of motion. All dimensions in mm. ϕ is the angle between the load and the main flexure.